Physics Letters A 375 (2011) 265–270

Contents lists available at ScienceDirect

Physics Letters A

www.elsevier.com/locate/pla

Resonant freak microwaves

F.M. de Aguiar *

Departamento de Física, Universidade Federal de Pernambuco, Recife, PE 50670-901, Brazil

ARTICLE INFO

Article history:
Received 28 September 2010
Received in revised form 13 December 2010
Accepted 14 December 2010
Available online 17 December 2010
Communicated by P.R. Holland

Keywords:
Freak waves
Microwave resonators
Disordered media

ABSTRACT

The Helmholtz equation describing transverse magnetic modes in a *closed* flat microwave resonator with 60 randomly distributed discs is numerically solved. At lower frequencies, the calculated wave intensity *spatially* distributed obeys the universal Porter–Thomas form if localized modes are excluded. A superposition of resonant modes is shown to lead to rare events of extreme intensities (freak waves) at localized "hot spots". The *temporally* distributed intensity of such a superposition at the center of a hot spot also follows the Porter–Thomas form. Branched modes are found at higher frequencies. The results bear resemblance to recent experiments reported in an *open* cavity.

1. Introduction

A freak or rogue wave is defined as a sudden, large and steep wave pulse whose height is at least 2.2 times the significant wave height (SWH) which, in turn, is defined as the average height in the largest third of waves in a wave train. In the ocean, the SWH of surface waves may routinely reach 10 meters in bad weather conditions. In such a rough sea state, steep walls of water with heights between 20 and 30 m may be formed without warning, thus posing a potentially destructive threat to ships and offshore oil rigs. Giant waves are expected and do occur in the presence of counter propagating warm and cold currents, but perhaps those do not qualify as freak waves because they are not as surprising. On the other hand, a *linear* superposition of random Fourier modes may result in rogue waves, but with a probability prohibitively small. Actually, satellite images demonstrate that these extreme events occur in high seas more often than the prediction of the linear model. Lately, several features of freak waves in both random oceanic sea states [1–3] and nonlinear optical fibers [4] have been successfully simulated by numerical solutions of the *nonlinear* Schrödinger equation.

In a recent paper, Höhmann et al. [5] reported interesting room-temperature experimental results on freak microwaves in the linear regime. The experiments in [5] have been performed in a flat rectangular resonator whose bottom plate supported 55 to 60 brass cones, randomly distributed, thus with a smooth potential which might play the analog role of depth variations in the sea bed. Each cone has diameter 2.5 cm and height 1.5 cm. The bare resonator has dimensions 36.0 cm × 26.0 cm × 2.0 cm, and is *open* along the perimeter. Besides "branching structures" in the stationary microwave flow through the resonator at high frequencies, the authors in [5] found so-called "hot spots", which were associated with large deviations from the Rayleigh's distribution at high intensity values. In this work, we consider a *closed* model version of the transmission experiments described in [5], namely, a closed two-dimensional rectangular cavity with the same in-plane dimensions (36.0 cm × 26.0 cm), with 60 small hard scattering disks randomly distributed in its interior. Numerical solutions of the underlying Helmholtz equation with Dirichlet boundary conditions are shown to exhibit intriguing similarities with the microwave experiments reported in [5].

Previously, localized modes in a disordered cavity have been extensively studied in microwave experiments by Sridhar and coworkers [6]. In particular, deviations from the Porter–Thomas distribution for the wave intensity in cavities with 36 and 72 scatterers were reported in [6a], which were attributed to localization. Here, all disks have the same diameter 0.6 cm and are assumed to have the same cavity thickness d. Thus, all modes are two-dimensional for frequencies $f < c/2d$, where c is the speed of light. One may include three-dimensional resonant modes, as did the authors in [5], but here we investigate the two-dimensional ones only, for simplicity. Assume d is small enough ($c/2d \sim 25$ GHz for $d = 6$ mm) and that the longer dimensions of the cavity lie in the x–y plane. Thus, it is well known that the z-component of the electric field for transverse magnetic modes in such a cavity obeys the Helmholtz equation [7,8]

$$\left(\frac{\partial^2}{\partial x^2} + \frac{\partial^2}{\partial y^2} + k^2\right) E_z(x, y) = 0, \tag{1}$$

* Tel.: +55 81 2126 8450 (ext.: 7619); fax: +55 81 3271 0359.
E-mail address: fma@df.ufpe.br.

0375-9601/
doi:10.1016/j.physleta.2010.12.036

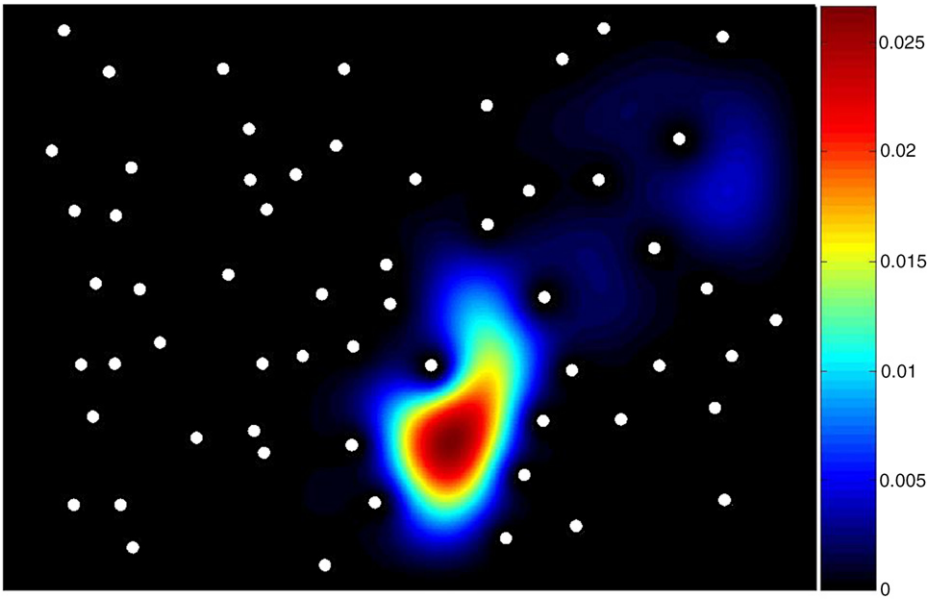

Fig. 1. Density plot of the numerically calculated microwave intensity $I \sim |E_z(x, y)|^2$, corresponding to the lowest eigenfrequency ($f = 2.346$ GHz) in a 26.0 cm $\times$ 36.0 cm two-dimensional resonator with 60 scattering disks (white dots) randomly distributed. Each disk has a diameter 0.6 cm. The color code on the right indicates the wave intensity in arbitrary units.

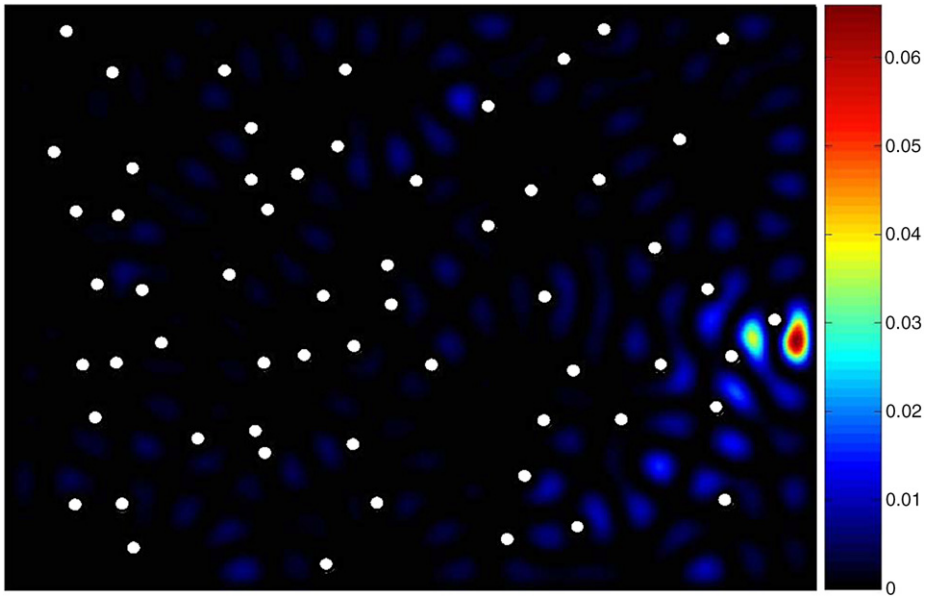

Fig. 2. Higher order ($n = 240$) resonating mode calculated at $f = 9.460$ GHz, exhibiting a "hot spot" close to the rightmost cavity border.

where $k = 2\pi f/c$, with boundary conditions, say, $E_z(x = 0, y) = E_z(x = 36.0 \text{ cm}, y) = E_z(x, y = 0) = E_z(x, y = 26.0 \text{ cm}) = 0$. E_z must also vanish at the border of each scattering disk. Solutions of Eq. (1) in this disordered medium were obtained with a finite element method previously used to simulate experiments in quantized billiards [9,10] and vertical cavity surface emitting lasers [11]. In the following, we refer to the intensity $I \sim |E_z(x, y)|^2$.

2. Numerical results and discussion

Fig. 1 shows the standing wave intensity pattern corresponding to the ground state at $f = 2.346$ GHz, displayed through 166,361 pixels. Let n denote the order of a solution of Eq. (1) ($n = 1$ for the ground state). For low values of n, most modes exhibit a localized nodal region, such as the one in Fig. 1. For a comparison with the experiments of Ref. [5], we have sought localized modes at higher frequencies, particularly when the wavelength becomes comparable to the mean distance between the scattering discs. A number of such modes were found for $n > 200$. In Fig. 2 we show the one with $n = 240$ and resonance frequency $f = 9.460$ GHz. In the same arbitrary scale of Fig. 1, where the localized peak in the ground state does not exceed an intensity of 0.03, at the center of the "hot spot" at the right-hand side in Fig. 2 one observes an intensity larger than 0.06. With the origin at the lower leftmost corner of the resonator, as suggested by the boundary conditions above, the center of the hot spot in Fig. 2 is located more precisely at $(x, y) = (35.000 \text{ cm}, 11.154 \text{ cm})$. We then followed the time evolution of the microwave intensity at that position when there are N modes simultaneously excited in the cavity. Following [5], we write such superposition as

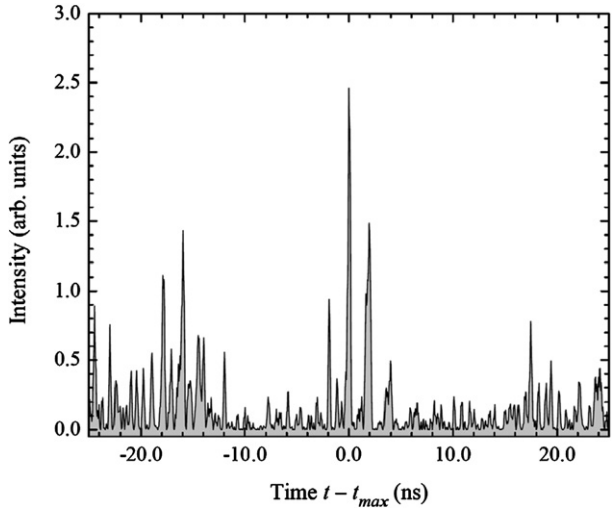

Fig. 3. A freak wave event at the center of the hot spot shown in Fig. 2, at time $t_{\max} = 23{,}201.35$ ns after the initial condition. Only waves with intensities larger than 1.86 qualify as freak waves in the long record. (Watch the behavior of the corresponding standing wave pattern in the video (Movie 1) in the online version at doi:10.1016/j.physleta.2010.12.036.)

$$\psi(x, y, t) = \sum_{j=1}^{N} E_z^{(j)}(x, y) \exp\bigl[i(2\pi f_j t + \phi_j)\bigr]. \tag{2}$$

Here, $E_z^{(j)}(x, y)$ is the solution of Eq. (1) at frequency f_j and ϕ_j is a random phase factor. Now the intensity $I \sim |\psi(x, y)|^2$. In the transmission experiments of Ref. [5], $N = 150$ stationary patterns have been used with randomly chosen frequencies normally distributed about the experimental hot spot frequency of 9.5 GHz. Here, we use $N = 70$ resonating modes randomly chosen about the calculated frequency of 9.460 GHz, corresponding to the hot spot shown in Fig. 2, with a standard deviation of 1 GHz. In a time series with 1,000,000 points, corresponding to an interval of 50,000 ns, we found 197,192 intensity peaks at the centre of the hot spot shown in Fig. 2. The average intensity in the largest third of that record was 0.385, in the same arbitrary units of Figs. 1 and 2. Multiplying this mean value by the factor $(2.2)^2 = 4.84$, we obtain the number 1.86, that might be regarded as the minimum intensity required for a "freak wave" event in that record. Based on this criterion, only 12 peaks among the 197,192 recorded qualify as rogue wave events. In Fig. 3 we show the one occurring at $t \equiv t_{\max} = 23{,}201.35$ ns after the initial condition, with an intensity of 2.460, about forty times the hot spot intensity peak shown in Fig. 2. In Movie 1 (the video can be found online at doi:10.1016/j.physleta.2010.12.036) we provide the time evolution of the intensity corresponding to that superposition in the whole cavity and in a time interval of a few nanoseconds centered in the freak wave event shown in Fig. 3. Notice that most of the 70 modes do not exhibit a pronounced localization feature at the position of the hot spot shown in Fig. 2. That is why only rarely a coherent superposition leads to extreme events at that position.

In order to compare the intensity distribution with existing formulae and experimental data, we need to normalize the intensity by dividing I by its mean value $\langle I \rangle$. Let $\tilde{I} = I/\langle I \rangle$ denote the normalized intensity. For an open system with a permanently radiating source, the intensity distribution of the traveling waves must obey the Rayleigh law [12a], namely,

$$P_R(\tilde{I}) = \exp(-\tilde{I}). \tag{3}$$

In closed disordered systems, a universal Porter–Thomas (PT) distribution

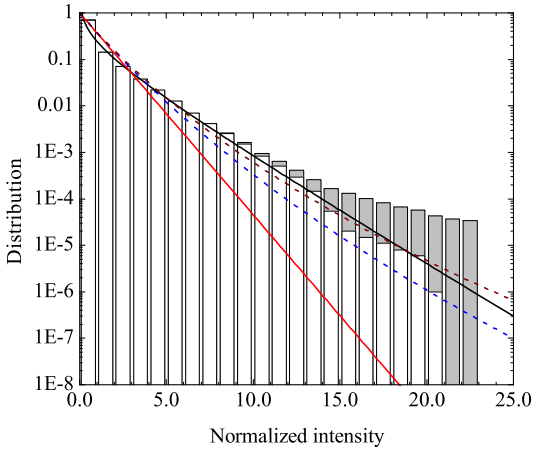

Fig. 4. Spatial intensity distribution calculated for 12 resonating modes in the interval 7.5 GHz $< f <$ 11.0 GHz. The gray histogram includes hot spots, which are absent in the white histogram. The red line is the Rayleigh law, the blue (brown) dashed line is drawn from Eq. (3) with $\gamma = 23.5$ (16.0). The black solid line is the Porter–Thomas distribution. (For interpretation of the references to color in this figure legend, the reader is referred to the web version of this Letter.)

$$P_{PT}(\tilde{I}) = \sqrt{\frac{1}{2\pi\tilde{I}}} \exp\left(-\frac{\tilde{I}}{2}\right) \tag{4}$$

is expected, provided "bouncing ball" modes and localized modes are excluded, as reported in microwave experiments in [6a] and confirmed in the numerical experiments here. In between, there is the important challenging class of disordered open systems. In 1998, Mirlin, Pnini and Shapiro (MPS) [12b] calculated a formula for the intensity distribution of monochromatic waves propagating in the particular case of a quasi-one-dimensional random medium that supports a point source and a point detector. The MPS formula, which has been used to fit microwave data in [5], reads

$$P_{MPS}(\tilde{I}) \propto \exp\left\{-\frac{\gamma}{2}\left[\ln^2\left(\sqrt{1+\frac{2\tilde{I}}{\gamma}} + \sqrt{\frac{2\tilde{I}}{\gamma}}\right)\right]\right\}, \tag{5}$$

where the parameter γ is proportional to the dimensionless conductance [12]. The grey histogram in Fig. 4 shows the calculated spatial intensity distribution for twelve representative modes of our resonator in the frequency interval between 7.5 and 11.0 GHz. This corresponds to ca. 2,000,000 pixels. Four of these modes are hot-spot like resonances, with local intensity peaks at different positions. The white histogram in Fig. 4 was also obtained from twelve modes, but with the four localized modes replaced by extended ones. Similarly to the experiments in [5], the hot-spot-free distribution goes downward. Here, as in the experiments in [6a], it approaches the universal PT distribution (black solid line in Fig. 4). For comparison, the red line in Fig. 4 is the Rayleigh law, the blue dashed line is the MPS distribution for $\gamma = 23.5$ (used to fit data in [5]), and the brown dashed line is the MPS formula with $\gamma = 16.0$. In principle, it might sound nonsense to use Eq. (5) to fit our data, given that we are dealing with a closed two-dimensional system. However, for arbitrary dimensionality d and large intensities, one might expect a decay slower than the PT result, through [12a]

$$P(\tilde{I}) \sim \exp\left[-\frac{\beta}{4\kappa}\ln^d(\kappa\tilde{I})\right], \tag{6}$$

where $\beta = 1$ (2, 4) for the orthogonal (unitary, symplectic) symmetry class of random matrix theory, and κ is proportional to the inverse of the conductance in both $d = 1$ and $d = 2$. Eq. (6), which

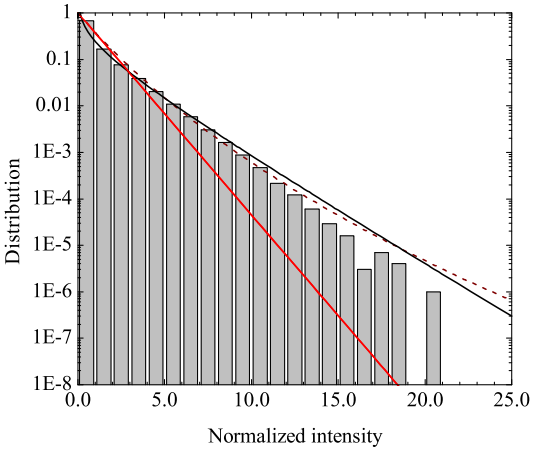

Fig. 5. Temporal intensity distribution calculated at the center of the hot spot in Fig. 2, for a random superposition of 70 resonant modes (Eq. (2)), and $0 < t < 50{,}000$ ns. As in Fig. 4, the red line is the Rayleigh law, and the brown dashed line is drawn from Eq. (3) with $\gamma = 16.0$. The black solid line is the Porter–Thomas distribution. (For interpretation of the references to color in this figure legend, the reader is referred to the web version of this Letter.)

is valid for $\tilde{I} \gtrsim \kappa^{-1}$, has a form analogous to the MPS formula at large intensities

$$P_{MPS}(\tilde{I} \gg \gamma) \cong \exp\left[-\frac{\gamma}{8}\ln^2\left(\frac{8}{\gamma}\tilde{I}\right)\right].$$

Thus, the behavior of our closed two-dimensional cavity might not be very far from the one expected for the disordered one-dimensional waveguide studied by MPS at large intensities.

By fixing the position at the center of the hot spot shown in Fig. 2, we find essentially the same distribution of intensities in a time sequence due to the linear superposition given in Eq. (2), with a downward deviation from the PT distribution at higher intensities, as shown in Fig. 5. In the long time series, $\langle I\rangle = 0.119$, so that in Fig. 3 $\tilde{I}_{\text{freak}} = I_{\text{freak}}/\langle I\rangle = 2.46/0.119 = 20.7$. That corresponds to the rightmost vertical bar in Fig. 5. This freak wave has less than half intensity of the one experimentally studied in [5], which was built with more than twice the number of modes used in the superposition here. Notice that most of the 70 modes in our superposition do not exhibit individually a localization feature at the hot spot position in Fig. 2. Thus, differently from the *spatial* intensity distribution, the hot spots do not exhibit a clear signature in the local *temporal* intensity distribution.

Localized modes in the disordered medium might play a role analogous to the solutions associated to periodic orbits in simple classically ergodic geometries. In order to observe the quantum signatures of chaos in the level dynamics in the semiclassical regime, one must eliminate these solutions from the spectrum, usually breaking all geometric symmetries in the boundary. Here, by excluding the localized modes, we somehow keep the modes that better reflect the classical ergodicity of the system, namely, the extended modes.

In the past ten years, scanning probe techniques allowed the imaging of electron flow in semiconductor devices, both in zero magnetic field and in the quantum Hall regime. The microwave experiments of Ref. [5] were primarily motivated by one of these results, namely, the observation of branches in images of electron flow in a high-mobility two-dimensional electron gas (2DEG) at low temperature and zero magnetic field [13]. These branches have been associated with small-angle scattering of the carriers by the random potential induced by ionized donor atoms, assumed to be fixed at cryogenic temperatures. Ray-tracing of the classical trajectories revealed branching structures similar to the observed ones. The same classical ray simulation was used in [5]. Here we show

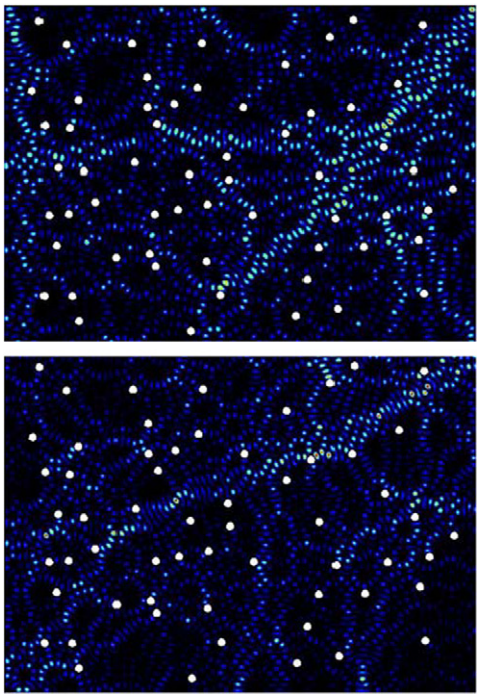

Fig. 6. Calculated branched modes in our two-dimensional cavity. Top: 33.04 GHz. Bottom: 35.69 GHz. These are to be compared with the measured standing microwave pattern shown in Fig. 2 of Ref. [5] at frequency 30.95 GHz.

that the observed microwave pattern observed in [5] might as well be compared with "branched" two-dimensional resonating modes. For instance, in Fig. 6 we show the standing wave patterns numerically calculated with eigenfrequencies 30.04 GHz (top panel) and 35.69 GHz (bottom panel). There are striking similarities between the two panels in Fig. 6 and the experimentally observed pattern at 30.95 GHz shown in Fig. 2 of Ref. [5]. One may observe there the presence of nodal lines, which are quite visible in both panels in Fig. 6. Notice that in the experiments by Topinka et al. [13], *fringes* at half the Fermi wavelength were observed in the images of the electron flow, thus underscoring the coherent wavelike nature of electron transport in the 2DEG.

Now we simulate the effect of moving a small antenna along a line segment in a channel between the scattering disks on both intensity and resonance frequency of the localized mode shown in Fig. 2. For that we add a smaller disk at initial position $(x_0, y_0) = (20.0\text{ m}, 11.0\text{ m})$ and move it rightwards along the line $y = 11.0$ m. The wave pattern of the hot-spot like mode closest to 9.460 GHz, for 15 frames in the interval $20.0\text{ m} \leqslant x \leqslant 29.0$ cm, where x is the horizontal coordinate of the "antenna", is shown in the Movie 2 that accompanies the online version of this Letter (the video can be found online at doi:10.1016/j.physleta.2010.12.036). In Fig. 7 we plot the highest intensity as a function of x for that particular hot spot, and in Fig. 8 the corresponding eigenfrequencies. While the intensity may vary by a factor of 3.3 along that line segment, there is only a small red shift (~ 40 MHz) in the resonance frequency in the vicinity of $x = 28.0$ cm. This might be relevant for transport experiments through a smooth potential, in which hot spots may disappear depending on the position of the antenna [5].

Another feature observed in the experiments described in [5] is the variation of the hot spot position as the frequency is swept. The transmission spectrum of the open cavity studied in [5] is not available. In the literature, broad resonances, with linewidth $\Delta f \sim 0.5$ GHz, were observed in scattering experiments through n-disk geometries around 10 GHz by Sridhar and co-workers [6b]. We take that as a reference. In our model, there are 20 eigenmodes of the cavity in the interval $\Delta f = 0.316$ GHz centered at

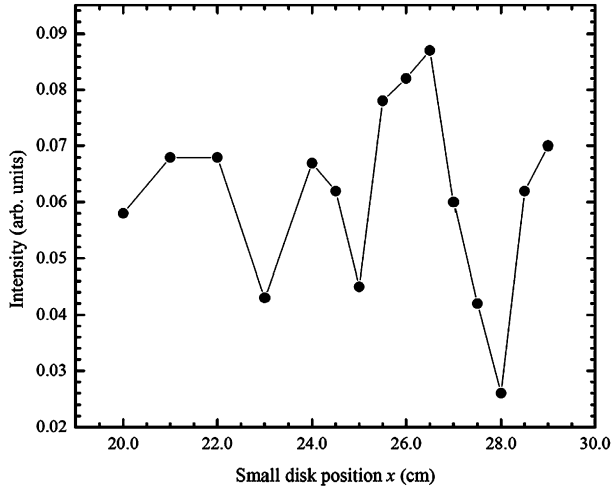

Fig. 7. Intensity fluctuation of the hot spot shown in Fig. 2, as an extra smaller disk moves along the line $y = 11.0$ cm on the segment defined by the interval 2.0 cm $\leqslant x \leqslant$ 29.0 cm. (Watch the behavior of the corresponding standing wave pattern in the Movie 2 in the online version at doi:10.1016/j.physleta.2010.12.036.)

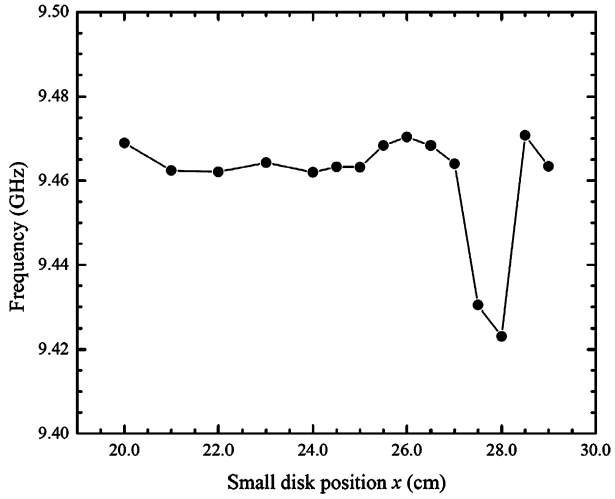

Fig. 8. Variation of the hot spot frequency, as an extra smaller disk moves along the line $y = 11.0$ cm on the segment defined by the interval 2.0 cm $\leqslant x \leqslant$ 29.0 cm. (Watch the behavior of the corresponding standing wave pattern in the Movie 3 in the online version at doi:10.1016/j.physleta.2010.12.036.)

9.460 GHz, the frequency of the "hot spot" in Fig. 2. The calculated eigenfrequencies in this range, in GHz, are: $f^{(1)} = 9.281$, $f^{(2)} = 9.288$, $f^{(3)} = 9.297$, $f^{(4)} = 9.347$, $f^{(5)} = 9.353$, $f^{(6)} = 9.363$, $f^{(7)} = 9.401$, $f^{(8)} = 9.419$, $f^{(9)} = 9.439$, $f^{(10)} = 9.460$, $f^{(11)} = 9.470$, $f^{(12)} = 9.487$, $f^{(13)} = 9.503$, $f^{(14)} = 9.523$, $f^{(15)} = 9.541$, $f^{(16)} = 9.543$, $f^{(17)} = 9.548$, $f^{(18)} = 9.581$, $f^{(19)} = 9.588$, and $f^{(20)} = 9.597$. In this regime of poor experimental resolution, a comparison with the microwave data might be made more realistically in terms of superpositions of the corresponding wavefunctions $E_z^{(n)}$. Here we consider, for instance, a wave packet comprised of five neighboring eigenfunctions with the form

$$E_z = \frac{1}{3}E_z^{(n-2)} + \frac{\sqrt{2}}{3}E_z^{(n-1)} + \frac{\sqrt{3}}{3}E_z^{(n)} + \frac{\sqrt{2}}{3}E_z^{(n+1)} + \frac{1}{3}E_z^{(n+2)}, \tag{7}$$

with $3 \leqslant n \leqslant 18$. The resulting intensity, $|E_z|^2$, as the frequency is swept in the interval 9.460 ± 0.158 GHz, is shown in the Movie 3 that accompanies the online version of this Letter (the video can be found online at doi:10.1016/j.physleta.2010.12.036). This calculation clearly demonstrates how the pronounced peak associated with the "hot spots" may persist in a broad frequency interval, and move from place to place as a result of the change of the eigenmodes that constitute the superposition, as the frequency is varied. This result is also in qualitative agreement with the observations reported in [5].

3. Conclusions

In sum, we have performed numerical experiments in a planar microwave cavity with tens of randomly distributed scatterers. We observe "hot spots" at lower frequencies, where a random superposition of resonant modes induces rare events of large amplitude pulses that might be regarded as freak waves. Temporal and spatial (ensemble) intensity distributions satisfactorily agree with the universal Porter–Thomas distribution of random matrix theory. Given that flat microwave resonators and two-dimensional infinite quantum wells are isomorphic, this might be seen as a quantum signature of ergodicity in a classically chaotic system. In addition, "branches" associated with resonating standing wave patterns are observed at higher frequencies. Finally, we demonstrate that a superposition of a few modes might explain the persistent and wandering behavior of "hot spots" in a frequency interval as large as 0.5 GHz. Most of these results are analogous with the experiments recently reported in Ref. [5] in an open microwave resonator. It is important to recall that the complex reflection coefficient Γ for a short microwave circuit ($\Gamma = -1$) and that for an open circuit ($\Gamma = +1$) are on the unit circle of a Smith chart, *i.e.*, both open and short circuits share the same magnitude $\rho_0 \equiv |\Gamma| = 1$. In other words, ideally, both have infinite *standing wave ratios* $\mathrm{VSWR} = (1+\rho_0)/(1-\rho_0)$. At present, it is not clear how that fact might have affected the transport experiments in [5], but given the qualitative similarities presented here, we believe that one might not entirely discard resonance phenomena as a possible physical mechanism for the experimental observations reported in [5]. Localized modes, either due to hard-walled scattering elements, such as the disks used here, or to smooth potentials, such as the cones used in [5], indicate us where we should expect to observe, with a better chance, a rare freak wave *pulse* resulting from a linear superposition of, say, N modes. That has been demonstrated in [5] for $N = 150$ and here for $N = 70$ modes, with lower intensities, but still satisfying the standard criterion for a rogue wave event. In this sense, the formation of such linear freak waves does not seem to depend strongly on the particular type of scatterer. On the other hand, as mentioned in the introduction, the threatening steep-wall "monster" waves more frequently observed in random oceanic sea states, seem to be better described by the nonlinear model, as reported in [1–4] and [14].

Acknowledgements

Discussions with J.R. Rios Leite, J. Treddicce and A.M.S. Macêdo are gratefully acknowledged. We thank the anonymous referees for useful comments and suggestions. This work has been supported by CNPq and FACEPE, Brazilian Agencies.

Appendix A. Supplementary material

Supplementary material related to this Letter can be found online at doi:10.1016/j.physleta.2010.12.036.

References

[1] M. Onorato, A.R. Osborne, M. Serio, S. Bertone, Phys. Rev. Lett. 86 (2001) 5831.
[2] M. Onorato, A.R. Osborne, M. Serio, Phys. Rev. Lett. 96 (2006) 014503.
[3] M. Onorato, T. Waseda, A. Toffoli, L. Cavaleri, O. Gramstad, P.A.E.M. Janssen, T. Kinoshita, J. Monbaliu, N. Mori, A.R. Osborne, M. Serio, C.T. Stanberg, H. Tamura, K. Trulsen, Phys. Rev. Lett. 102 (2009) 114502.

[4] D.R. Solli, C. Ropers, P. Koonath, B. Jalali, Nature (London) 450 (2007) 1054.
[5] R. Höhmann, U. Kuhl, H.-J. Stöckmann, L. Kaplan, E.J. Heller, Phys. Rev. Lett. 104 (2010) 093901.
[6] (a) A. Kudroli, V. Kidambi, S. Sridhar, Phys. Rev. Lett. 75 (1995) 822;
(b) W. Lu, M. Rose, K. Pance, S. Sridhar, Phys. Rev. Lett. 82 (1999) 5233;
(c) P. Pradhan, S. Sridhar, Phys. Rev. Lett. 85 (2000) 2360.
[7] S. Sridhar, D. Hogenboom, B.A. Willemsen, J. Stat. Phys. 68 (1992) 239.
[8] H.-J. Stöckmann, Quantum Chaos – An Introduction, Cambridge University Press, Cambridge, 1999.
[9] D.D. de Menezes, M. Jar e Silva, F.M. de Aguiar, Chaos 17 (2007) 023116.
[10] F.M. de Aguiar, Phys. Rev. E 77 (2008) 036201.
[11] T.-D. Lee, C.-Y. Chen, Y. Lin, M.-C. Chou, T. Wu, R.-K. Lee, Phys. Rev. Lett. 101 (2008) 084101.
[12] (a) A.D. Mirlin, Phys. Rep. 326 (2000) 259;
(b) A.D. Mirlin, R. Pnini, B. Shapiro, Phys. Rev. E 57 (1998) R6285.
[13] M.A. Topinka, B.J. LeRoy, R.M. Westerwelt, S.E.J. Shaw, R. Fleischmann, E.J. Heller, K.D. Maranowski, A.C. Gossard, Nature (London) 410 (2001) 183.
[14] A.I. Dyachenko, V.E. Zakharov, JETP Letters 81 (2005) 255.